INSTITUTE OF PHYSICS PUBLISHING MEASUREMENT SCIENCE AND TECHNOLOGY

Meas. Sci. Technol. **17** (2006) R55–R70 doi:10.1088/0957-0233/17/6/R01

**REVIEW ARTICLE**

# Frequency domain complex permittivity measurements at microwave frequencies

**Jerzy Krupka**

Department of Electronics and Information Technology, Institute of Microelectronics and Optoelectronics, Warsaw University of Technology, Koszykowa 75, 00-662 Warszawa, Poland

E-mail: krupka@imio.pw.edu.pl

Received 16 May 2005, in final form 17 August 2005
Published 26 April 2006
Online at stacks.iop.org/MST/17/R55

**Abstract**
Overview of frequency domain measurement techniques of the complex permittivity at microwave frequencies is presented. The methods are divided into two categories: resonant and non-resonant ones. In the first category several methods are discussed such as cavity resonator techniques, dielectric resonator techniques, open resonator techniques and resonators for non-destructive testing. The general theory of measurements of different materials in resonant structures is presented showing mathematical background, sources of uncertainties and theoretical and experimental limits. Methods of measurement of anisotropic materials are presented. In the second category, transmission–reflection techniques are overviewed including transmission line cells as well as free-space techniques.

**Keywords:** frequency domain measurements, microwave measurements, permittivity, permeability, dielectric losses, magnetic losses

## 1. Introduction

One of the most widely known books on dielectric measurement is that of Von Hippel [1] published more than 50 years ago. A number of review papers, books [2–4] and hundreds of journal papers on this topic have been published since that time but still readers may find it difficult to choose an appropriate measurement technique to satisfy their measurements needs. In this paper, an overview of measurement techniques applicable for measurements of the complex permittivity of various materials at microwave frequencies is presented.

In the frequency domain the complex permittivity of any linear material is generally defined as a tensor quantity describing the relationship between the electric displacement ($\vec{D}$) and the electric field ($\vec{E}$) vectors

$$\vec{D} = \overleftrightarrow{\varepsilon}\vec{E}. \tag{1}$$

For passive reciprocal materials such as ionic dielectric single crystals the permittivity tensor is symmetric and can be diagonalized which means that in a certain specific coordinate system it takes the diagonal form

$$\overleftrightarrow{\varepsilon} = \begin{bmatrix} \varepsilon_{11} & 0 & 0 \\ 0 & \varepsilon_{22} & 0 \\ 0 & 0 & \varepsilon_{33} \end{bmatrix}. \tag{2}$$

For polycrystalline materials, glasses, plastics and some crystals (e.g., having cubic crystallographic structure) all diagonal elements become identical and the complex permittivity becomes a scalar quantity. The complex permittivity of an isotropic material in general can be written as

$$\varepsilon = \varepsilon_0\varepsilon_\mathrm{r} = \varepsilon_0\left(\varepsilon_\mathrm{r}' - \mathrm{j}\varepsilon_\mathrm{rd}'' - \mathrm{j}\frac{\sigma}{\omega\varepsilon_0}\right) = \varepsilon_0\varepsilon_\mathrm{r}'(1 - \mathrm{j}\tan\delta) \tag{3}$$

where $\tan\delta$ is the total dielectric loss tangent given by

$$\tan\delta = \tan\delta_\mathrm{d} + \frac{\sigma}{\omega\varepsilon_0\varepsilon_\mathrm{r}'} \tag{4}$$

where $\varepsilon_\mathrm{r}$ is the relative complex permittivity, $\omega$ is the angular frequency, $\sigma$ is the conductivity, $\varepsilon_0 = 1/(c^2\mu_0) \approx 8.8542 \times 10^{-12}$ (F m$^{-1}$) denotes permittivity of vacuum and $\tan\delta_\mathrm{d}$ is the

dielectric loss tangent associated with all other dielectric loss mechanisms except conductivity.

The dielectric loss tangent of any material describes quantitatively dissipation of the electric energy due to different physical processes such as electrical conduction, dielectric relaxation, dielectric resonance and loss from nonlinear processes (such as hysteresis) [5]. When we measure the loss of a dielectric at a single frequency we cannot, in general, distinguish between them. Phenomenologically, they all give rise to just one measurable quantity, namely, the total measured loss tangent. The origin of dielectric losses can also be considered as being related to the time delay between the electric field and the electric displacement vectors.

For some materials like superconductors conductivity itself contains two terms: real (conductivity related to normal current) and imaginary (conductivity related to supercurrent). It is easy to prove that conductivity related to the supercurrent can be formally treated as a negative real permittivity. Similar phenomena take place in metals and semiconductors at very high frequencies (infrared and optical). From a measurement point of view materials such as dielectrics, metals and semiconductors can be characterized by the complex permittivity. The only differences between these materials at microwave frequencies are related to the values of real and imaginary parts of permittivity. For example, for metals the imaginary part of permittivity is many orders of magnitude larger than the real one while for dielectrics usually the real part is larger than the imaginary one.

Some materials commonly used at microwave frequencies such as ferrites exhibit magnetic properties that must be considered in measurements of their permittivity. The permeability tensor $\mu$ describes relationship between the magnetic induction $\vec{B}$ and magnetic field $\vec{H}$ vectors (1):

$$\vec{B} = \ddot{\mu}\vec{H}. \tag{5}$$

The most important microwave applications of ferrites are related to their non-reciprocal properties. In the presence of static magnetic field magnetizing ferrite material along $z$-axis of Cartesian or cylindrical coordinate system permeability of ferrite material is represented by Polder's tensor (6) [6]. Off-diagonal components of Polder's tensor are purely imaginary but they do not describe any magnetic losses since they appear with opposite signs. If ferrite material is lossy then particular tensor components ($\mu, \kappa, \mu_z$) become complex:

$$\overleftrightarrow{\mu} = \mu_0 \begin{bmatrix} \mu & \mathrm{j}\kappa & 0 \\ -\mathrm{j}\kappa & \mu & 0 \\ 0 & 0 & \mu_z \end{bmatrix}. \tag{6}$$

In addition to the intrinsic material properties defined above, we must concern ourselves with the extrinsic quantities we encounter in measurements of samples in different measurement cells. At microwave frequencies the size of measurement cells can be smaller, comparable or larger than the wavelength. In the first case, a measurement cell containing a sample under test can be treated as a lumped impedance circuit. In such a case the measured quantity is the complex impedance (or the complex admittance) and measurements are usually performed using impedance analysers. At higher frequencies external parameters are the complex reflection and/or the complex transmission coefficients and their measurements are usually performed using vector network analysers. The second group of measurement techniques is often called wave techniques. Both lumped impedance and wave techniques can be employed in resonators. Resonators are measurement cells with resonating electromagnetic fields inside them that are used to obtain high sensitivity for measuring the loss of low-loss dielectrics. Various wave techniques are used to measure the complex permittivity. Differences between techniques are related to both the cells used for measurements and mathematical models describing relationships between quantities that are directly measured (e.g., transmission and reflection coefficients) and the complex permittivity. Choice of a specific technique depends on several parameters such as frequency, size and shape of available samples, range of dielectric losses and presence of anisotropy.

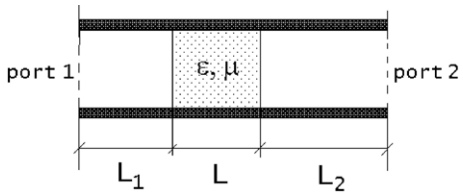


**Figure 1.** Transmission line measurement cell.

## 2. Transmission-line and free-space methods

Transmission and reflection methods are based on measurements of transmitted and/or reflected electromagnetic power from a sample under test illuminated by a well-determined incident electromagnetic wave. If the material of the sample is isotropic then determination of the complex permittivity and the complex permeability is possible from two measured parameters: the complex reflection ($S_{11}$) and the complex transmission ($S_{21}$) coefficients. For non-magnetic materials the complex permittivity can be derived only from one measured complex parameter (either $S_{11}$ or $S_{21}$). Transmission–reflection measurements can be performed employing closed measurement cells, open-ended probes but can also be undertaken in a free-space environment.

### *2.1. Coaxial and waveguide cells*

At frequencies below millimetre waves the sample under test is often situated in a measurement cell made as a short section of coaxial line, e.g., [7–9] or waveguide as shown in figure 1. There are published standard methods for the transmission-line technique: ASTM D5568–01 [10] and UTE (Union Technique de l'Electricité) [11]. ASTM D5568–01 standard presents a full procedure for transmission-line measurements, including measurements on magnetic materials and measurements in waveguide. The UTE standard [11] is for coaxial measurements on thin specimens in a special coaxial-line cell. Specimens are machined to the same length as the cell. To mitigate the air gap problem, the gaps are filled using a low-melting-point alloy. In determination of material properties one has to know the relationship between measurable quantities such as the complex reflection and the complex transmission coefficients, dimensions of the cell and sample and the complex permittivity of the sample.

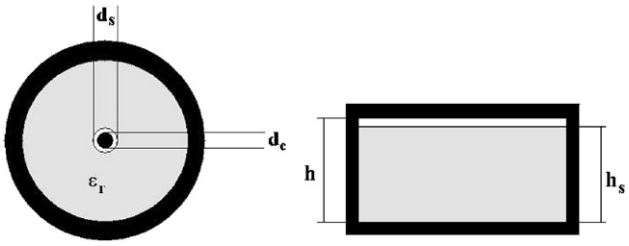


**Figure 2.** Transmission lines containing samples having dimensions smaller than their cross section.

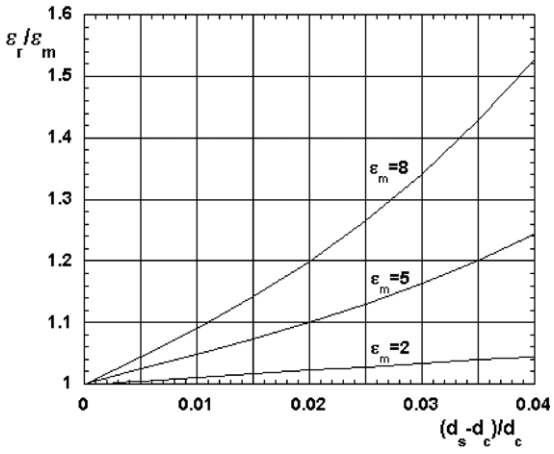


**Figure 3.** Ratio of the actual (real) permittivity of a sample to the measured permittivity versus relative gap value between sample and inner conductor of coaxial cell.

This requires solutions of Maxwell's equations for the cell containing the sample. Exact solutions are available for a few simple shapes of transmission lines when the sample under test occupies their whole cross section between two planes perpendicular to the line (e.g., for the structure shown in figure 1). When this condition is not satisfied, only numerical solutions of Maxwell's equations are available. Computations based on exact solutions usually employ explicit Nicolson and Ross expressions for the complex permittivity [7], but they can be unstable producing erroneous results when the length of the specimen is close to one or more half-wavelengths in the medium of the dielectric. Paper [12] presents an explicit algorithm which is believed to be more stable. An alternative approach uses iterative algorithms [13].

Transmission/reflection techniques are especially useful for broad frequency band measurements of lossy dielectric liquids [14]. Measurements of solid materials are more difficult, especially those having large permittivities. This is associated with the presence of air gaps between sample and metal parts of the measurement cells as shown in figure 2. The electric field for the TEM mode of coaxial cell is perpendicular to metal–dielectric interfaces and in the presence of air gaps becomes discontinuous. In most cases air gaps are non-uniform and very difficult to be measured and therefore to be accounted for. When the gap is neglected in electromagnetic analysis it causes substantial errors in permittivity determination. In figure 3 quantitative permittivity errors are shown versus relative gap values between inner conductor and a dielectric sample. One can notice that relative permittivity errors increase with increasing

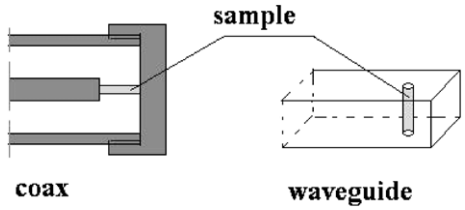


**Figure 4.** Coaxial and waveguide cells used for measurements of high permittivity materials. To minimize air gap influence both ends of samples are metallized.

gap and permittivity values. In order to mitigate errors associated with air gaps solid samples are often metallized or covered with conductive pastes or solders (as in [11]), but this usually creates additional errors in dielectric loss tangent determination.

Although in principle measurements in coaxial lines employing TEM mode can be performed up to very high frequencies, in practice, they are rarely performed at frequencies higher than 10 GHz. Reasons for this are decrease of measurement accuracy related to smaller size of samples (their length should be smaller than half the wavelength to avoid resonances in the sample), increase in parasitic losses and increasing influence of imperfections in measurement systems on determination of the complex permittivity. More information on this topic can be found in [4]. The waveguide transmission line method has similar accuracy and resolution as the coaxial transmission line method but it is typically used at higher operating frequencies (lower frequency is always limited by the cut-off frequency of a specific waveguide). One of its advantages over the coaxial transmission line method is lack of an inner conductor which makes the air gap problem less critical. On the other hand, the frequency coverage for the waveguide transmission line method is smaller than for the coaxial counterpart and requires additional equipment like coax-waveguide adapters when used with modern network analysers. Measurements of high permittivity materials, such as ferroelectrics using samples that fully occupy cross section of coaxial line or waveguide become inaccurate due to high impedance mismatch between the sample and air filled sections of the transmission line. For measurements of ferroelectrics the cells shown in figure 4 are used [15, 16]. For such cells exact solutions of Maxwell's equations are not available so numerical techniques of electromagnetic analysis must be used to find the relationship between transmission and reflection coefficients and the complex permittivity. The upper measurement frequency limit for the coaxial cell shown in figure 4 is about 1 GHz for materials having permittivities of the order of a few thousands.

The main features of the guided transmission line technique can be summarized as follows:

*Advantages*

- Relatively broadband frequency coverage;
- Suitable for measurements of magnetic materials (ferrites);
- One of the best techniques at microwave frequencies for high loss and medium loss samples. Uncertainties for real permittivity better than $\pm 1\%$.

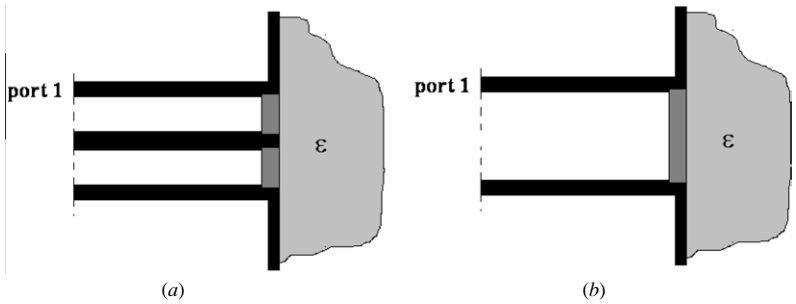


**Figure 5.** Open transmission line measurement cells: (*a*) coaxial and (*b*) waveguide.

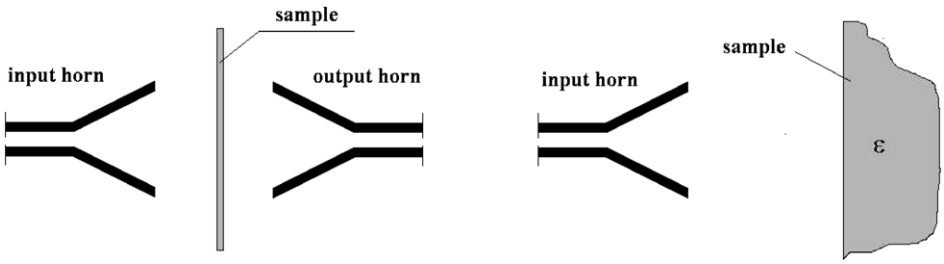


**Figure 6.** Schematic diagram of arrangements for free-space transmission/reflection or reflection measurements.

*Disadvantages*

- For solid specimens significant errors caused by air gaps;
- Limited resolution of loss tangent measurements (typically $\pm 0.01$).

### 2.2. Open-ended probes

One of the best techniques for measurements of lossy dielectrics (especially biological tissues) is an open-ended transmission line probe [17–24] schematically depicted in figure 5. This technique is applicable for measurements of non-magnetic materials. Since for open-ended transmission line geometry exact solutions of Maxwell's equations are not available, the complex permittivity is determined from measurements of the complex reflection coefficient $S_{11}$ employing one of the rigorous techniques of electromagnetic analysis such as mode matching, finite element of finite difference. A single coaxial probe can typically operate over a frequency range of about 30:1 with uncertainty for real permittivity order of $\pm 3\%$ for suitable materials. The frequency range depends on the diameter of the coaxial aperture and, e.g., a coaxial probe with 7 mm aperture can operate from 200 MHz to 6 GHz. The best measurements accuracy and resolution is achieved around the centre frequency of this band. Smaller probes can cover appropriately higher frequencies but measurement uncertainties typically increase with increasing frequency. In measurements of solids the air gap problem is important but it can be mitigated by pressing the probe against a flat surface of the sample under test. It is only helpful if the sample is relatively soft.

Open-ended waveguide probes [20–24] are used less often than coaxial probes, partly because they are limited in frequency range and at lower frequencies they are physically large. Waveguide probes offer two advantages over coaxial probes for specific applications. First, such probes are better matched for measuring lower permittivity than coaxial probes of similar size and at a similar frequency. Second, they can be used for measurements of anisotropic materials since the electric field for the dominant mode of rectangular waveguide is linearly polarized. Two permittivity tensor components of uniaxially anisotropic material can be derived by carrying out two measurements on the flat face of the specimen, with the specimen orientated in two orthogonal directions: one parallel to the anisotropy axis and the other perpendicular to the anisotropy axis. A full numerical analysis that takes into account permittivity as a tensor must be performed in order to evaluate properly the two permittivity components [24]. In all other respects waveguide probes are similar to coaxial probes.

Advantages of coaxial and waveguide open-ended probe techniques:

- Quick, easy and relatively cheap to use compared with other methods;
- A single probe can be used over a frequency range of 30:1 with suitable samples;
- Well-suited for non-destructive testing.

Disadvantages of coaxial and waveguide open-ended probe techniques:

- Air gaps between specimens and probes are difficult to avoid with hard solid specimens;
- Difficult calibration;
- The methods are generally less accurate than techniques described in the previous section with typical uncertainties of $\pm 3\%$ for real permittivity.

### 2.3. Free-space measurements of the complex permittivity

At millimetre wave frequencies instead of transmission line cells and open-ended probes, free-space measurements are used. Measured quantities are again the complex scattering matrix coefficients (transmission, reflection or both) measured on a sample under test situated between two antennas or in front of one antenna as shown in figure 6. One of the requirements

for accurate free-space measurements is that the size of the samples under test in the direction perpendicular to the incident wave is larger than the electromagnetic beam width, so diffraction from the edges of samples can be neglected.

Free electromagnetic fields are typically radiated as beams from antennas. In the unfocused-beam methods electromagnetic energy creates diverging beams, so corrections for attenuation of the beam between transmitting and receiving antennas have to be incorporated in the method. The beam typically extends beyond the aperture of the receiving antenna at relatively short distance and may also spread beyond the aperture of the sample. Such methods are therefore prone to errors caused by diffraction at antennas and sample edges. For this reason focused-beam methods are more often used in practice. Dielectric lenses or concave mirrors are used to focus the beam. The most commonly used calculable beam is the Gaussian beam [24, 25] that can be radiated from corrugated-horn antennas [26, 27]. For a Gaussian beam, electromagnetism decays exponentially (in the manner described by the Gaussian function) in the radial direction with maximum magnitude at the axis of beam propagation, so diffraction problems may be made negligible. The practical ability to focus Gaussian beams improves as the frequency increases up to the terahertz region. At sufficiently high frequencies quasi-optical methods essentially become optical methods. Normal-incidence unfocused reflection and transmission have been used by a number of researchers for measuring large-area laminar specimens (see, e.g., [28] for a review). The measurements can be easily performed by using matched waveguide horns attached via coaxial cables to a network analyser, although in the past accurate measurements were performed with less advanced equipment such as waveguide bridges [29]. Computation of transmission and reflection coefficients is simple, assuming a plane-wave approximation, and such an approximation becomes more accurate as frequency increases. By rotating the sample about an axis perpendicular to the direction of propagation one can perform measurements at the Brewster angle of incidence [31]. Measurements can also be performed as a function of the angle of incidence [32]. Such measurements are often more accurate than those performed at normal incidence. In recent years, focused reflection and transmission methods have been improved by full understanding of the theory of corrugated-horn antennas and advances in their manufacturing. Complete measurement systems for laminar specimens have been constructed either with mirrors [33] or lenses [34] for focussing. Such systems are commercially available at frequencies from 1.5 GHz up to the sub-millimetre region of the spectrum. A typical measurement system is shown in figure 7.

The sample under test is situated in the narrowest part of the Gaussian beam where the beam is approximated by a plane wave. Such approximation introduces some errors because the Gaussian beam wavelength is not exactly the same as that of a plane wave at the same frequency. Free-space techniques are generally less accurate than their guided-wave equivalents and the focused methods are slightly more accurate than the unfocused ones. It is difficult to assess uncertainties quantitatively but according to [4] they lie in the range $\pm$(1–10)% for real permittivity and from $\pm$5% to over 20% for dielectric losses.

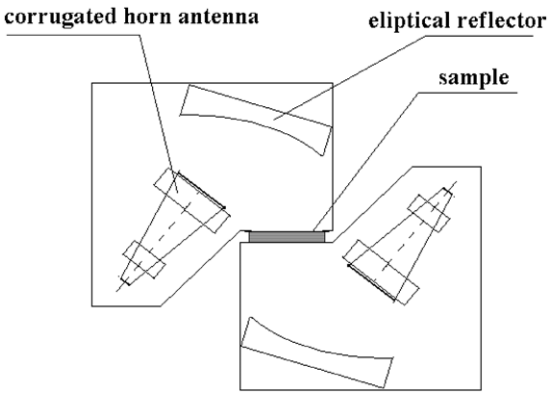


**Figure 7.** A quasi-optical focused beam technique for measuring the dielectric properties of a laminar sample at normal incidence.

Major areas of application of transmission and reflection methods described in section 2 are measurements of medium to high loss isotropic materials as a function of frequency. Some of these techniques (those where the electric field is linearly polarized) allow measurements of the complex permittivity for anisotropic materials.

## 3. Resonance methods

Resonators and cavities form a special class of measurement cells that are especially useful for measurements of very low loss materials, but they also offer the highest possible accuracy of measurements of real permittivity. Resonant methods can be divided into two categories. The first category includes different kinds of resonant cavities (including re-entrant cavities, cylindrical and rectangular cavities), open resonators and resonators loaded with a dielectric (e.g., split post dielectric resonators). For the second category the sample under test, itself, can create a dielectric resonator. Resonant methods employing cavities [35–44] and open resonators [45–52] operating at a single, dominant or a higher order well-established mode have been used for measurement of dielectric materials for more than 60 years. In a resonant cavity the electric energy stored in the sample under test is usually small compared to the total electric energy stored in the whole cavity (except re-entrant cavities [43, 44]). In the second category, a cylindrical or spherical dielectric sample under test, enclosed in a metal shield or situated in an open space, constitutes a dielectric resonator, where the resonance frequencies predominantly depend on permittivity and dimensions of the sample. In the dielectric resonator techniques, typically more than 90% of the total electric energy is stored in the sample. Progress in measurements of dielectrics employing resonant techniques during the last decades has been associated with two factors: the development of new low-loss dielectric materials and the advances in rigorous techniques of electromagnetic field computations. Using new low-loss dielectric materials it was possible to construct resonators filled with dielectrics that have higher $Q$-factors and better thermal stability than traditional all-metal cavities. Developments in electromagnetic field simulations have made it possible to construct resonant structures without restrictions on sample size or shape and also to obtain high accuracy with measurements.

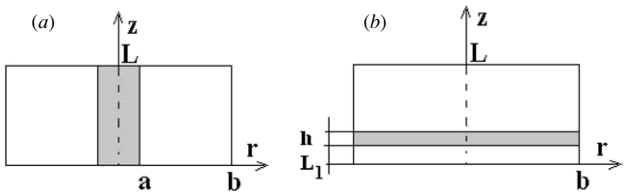


**Figure 8.** Cylindrical cavities: (*a*) containing a dielectric rod and (*b*) containing a dielectric disc.

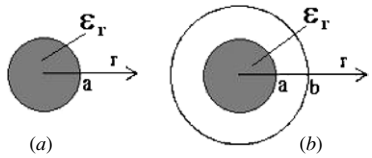


**Figure 9.** Spherical resonators: (*a*) a dielectric sphere in a free space and (*b*) a spherical cavity containing a dielectric sphere.

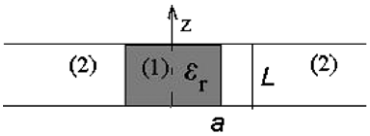


**Figure 10.** Cylindrical dielectric resonator between conducting planes.

### *3.1. General concepts of measurements by resonance methods*

Measured quantities in resonance techniques are the resonant frequency and the $Q$-factor of a specific mode excited in the resonant structure containing the sample under test. The complex permittivity of the sample can be evaluated from these two measured quantities provided all other parameters of the structure are known. These parameters include dimension of the structure, surface resistance of metal parts, coupling coefficients, radiation losses and the complex permittivities of dielectric supports (if present). Exact relations between permittivity, sample and cavity dimensions, and measured resonant frequency and the unloaded $Q$-factor can only be derived if resonant structures that permit theoretical analysis by separation of variables are used. Practically, this is only possible when the measurement system has simple cylindrical, spherical or rectangular geometry and where any permittivity inhomogeneity in the measured structure exists in only one of the principal coordinate directions and all conductive surfaces are made of perfect conductors. Examples of such geometries are shown in figures 8–10. For these geometries transcendental equations can be derived that represent relationship between the complex permittivity and the complex angular frequencies of a specific resonant structure. The general form of such an equation can be written as

$$F(\varepsilon_{\mathrm{r}}, \omega) = 0, \tag{7}$$

where $\mathrm{Re}(\omega) = 2\pi f$, $\mathrm{Im}(\omega) = \mathrm{Re}(\omega)/2/Q_{\mathrm{d}}$ and $Q_{\mathrm{d}}$ is the $Q$-factor depending on dielectric losses and radiation losses in the resonant structure.

Strictly transcendental equations can be derived if metal wall losses and coupling losses are assumed to be zero, but these extra losses are also taken into account in the complex permittivity determination. This problem will be discussed later on. Examples of transcendental equations that are commonly used in measurements of dielectric properties and that are important for understanding the mathematical description of different physical phenomena in resonant structures are given below.

The transcendental equation for $\mathrm{TE}_{01p}$ modes of a cylindrical cavity [41] is shown in figure 8(*b*) for $L_1 = 0$.

$$k_{z0}\tan(k_z h) + k_z \tan[k_{z0}(L-h)] = 0, \tag{8}$$

where $k_{z0}^2 = (\omega/c)^2 - (u'_{01}/b)^2$, $k_z^2 = (\omega/c)^2\varepsilon_{\mathrm{r}} - (u'_{01}/b)^2$ and $u'_{01}$ is the first root of the derivative of Bessel function of the first kind and zero order $u'_{01} = 3.831\,71$.

The transcendental equation for all modes in a parallel plate cylindrical dielectric resonator [53] is

$$\left[\frac{\varepsilon_{\mathrm{r}} J'_{\mathrm{m}}(k_{\rho 1}a)}{k_{\rho 1}a J_{\mathrm{m}}(k_{\rho 1}a)} - \frac{H'^{(2)}_{\mathrm{m}}(k_{\rho 2}a)}{k_{\rho 2}a H^{(2)}_{\mathrm{m}}(k_{\rho 2}a)}\right] \times \left[\frac{J'_{\mathrm{m}}(k_{\rho 1}a)}{k_{\rho 1}a J_{\mathrm{m}}(k_{\rho 1}a)} - \frac{H'^{(2)}_{\mathrm{m}}(k_{\rho 2}a)}{k_{\rho 2}a H^{(2)}_{\mathrm{m}}(k_{\rho 2}a)}\right] = \frac{m^2 k_z^2}{k_2^2}\left[\frac{1}{(k_{\rho 1}a)^2} - \frac{1}{(k_{\rho 2}a)^2}\right], \tag{9}$$

where

$$k_1^2 = \frac{\omega^2}{c^2}\varepsilon_{\mathrm{r}} \qquad k_2^2 = \frac{\omega^2}{c^2}$$
$$k_{\rho 1}^2 = k_1^2 - k_z^2 \qquad k_{\rho 2}^2 = k_2^2 - k_z^2$$
$$k_z^2 = \frac{p\pi}{L}.$$

The transcendental equation for $\mathrm{TE}_{n0p}$ modes of a dielectric sphere in free space [54] is

$$\varepsilon_{\mathrm{r}}^{1/2} J_{n-1/2}(ka) H^{(2)}_{n+1/2}(k_0 a) - J_{n+1/2}(ka) H^{(2)}_{n-1/2}(k_0 a) = 0, \tag{10}$$

where

$$k = \frac{\omega}{c}\sqrt{\varepsilon_{\mathrm{r}}},\ k_0 = \frac{\omega}{c}$$

and $J$ and $H^{(2)}$ denote Bessel's and Hankel's functions.

The transcendental equation for $\mathrm{TE}_{n0p}$ modes of a dielectric sphere in a spherical cavity [54] is

$$\begin{aligned}\varepsilon_{\mathrm{r}}^{1/2} J_{n-1/2}(ka)&[J_{n+1/2}(k_0 a) Y_{n+1/2}(k_0 b) - Y_{n+1/2}(k_0 a) J_{n+1/2}(k_0 b)] \\ &- J_{n+1/2}(ka)[J_{n-1/2}(k_0 a) Y_{n+1/2}(k_0 b) - Y_{n-1/2}(k_0 a) J_{n+1/2}(k_0 b)] = 0.\end{aligned} \tag{11}$$

*3.1.1. Q-factors and parasitic losses in resonant structures.* The $Q$-factor of a resonant structure, for any mode of operation, is associated with different kinds of losses such as dielectric losses ($Q_{\mathrm{d}}$), conductor losses ($Q_{\mathrm{c}}$), radiation losses ($Q_{\mathrm{r}}$) and coupling losses ($Q_{\mathrm{coupling}}$). Particular $Q$-factors are related by the well-known formulae (12)–(16):

$$Q^{-1} = Q_{\mathrm{d}}^{-1} + Q_{\mathrm{c}}^{-1} + Q_{\mathrm{r}}^{-1} + Q_{\mathrm{coupling}}^{-1} \tag{12}$$

$$Q_{\mathrm{d}}^{-1} = \sum_{i=1}^{I} p_{ei} \tan\delta_i \tag{13}$$

$$Q_{\mathrm{c}}^{-1} = R_{\mathrm{S}}/G \tag{14}$$

where $Q$ is the total $Q$-factor of the resonant structure, $R_S$ is the surface resistance of the metal shield at a given resonant frequency, $G$ is the geometric factor of the shield, $p_{ei}$ is the electric energy filling factor for the $i$th dielectric region.

The geometric factor $G$ and electric energy filling factors $p_{ei}$ are defined as follows:

$$G = \omega \frac{\iiint_{V_t} \mu_0 |\mathbf{H}|^2 \, \mathrm{d}v}{\iint_S |\mathbf{H}_\tau|^2 \, \mathrm{d}s} \tag{15}$$

$$p_{ei} = \frac{\iiint_{V_d} \varepsilon_i |\mathbf{E}|^2 \, \mathrm{d}v}{\iiint_{V_t} \varepsilon(v) |\mathbf{E}|^2 \, \mathrm{d}v} \tag{16}$$

where $V_d$ is the volume of dielectric resonator, $V_t$ is the volume of whole resonant structure, $\varepsilon(v)$ is the spatially dependent permittivity inside the whole resonant structure and $\varepsilon_i$ is the permittivity of $i$th dielectric region.

For low-loss materials electric energy filling factors can be alternatively determined from incremental frequency rules, that require computations of the derivative of the resonant frequency with respect to the real permittivities of dielectric regions [55]. For cylindrical $TE_0$ mode resonant structures having axial symmetry an incremental frequency rule can also be used to determine geometric factor [56]. In this case derivatives are to be computed with respect to cavity wall perturbations.

Coupling losses are usually determined experimentally. For a resonator with two coupling ports the relationship between the total $Q$-factor (or loaded $Q$-factor), the unloaded $Q$-factor ($Q_u$) and coupling coefficients ($\beta_1$ and $\beta_2$) is given by the formula

$$Q_u^{-1} = Q_d^{-1} + Q_c^{-1} + Q_r^{-1} = \frac{Q^{-1}}{1 + \beta_1 + \beta_2}. \tag{17}$$

The unloaded $Q$-factor can be determined either if coupling coefficients are known from measurements or if they both are at least two orders of magnitude smaller than unity. In the last case one can assume within experimental errors that the unloaded $Q$-factor is the same as the total measured $Q$-factor. The $Q$-factor due to conductor losses can be evaluated from equations (14) and (15) providing that the magnetic field distribution for a specific mode of interest in the resonant structure and the surface resistance of metal shield are known. For close resonant structures radiation losses are equal to zero, so the $Q$-factor due to dielectric losses can be determined from the measured unloaded $Q$-factor value subtracting the part depending on conductor losses using equation (17). Then the complex angular frequency can be evaluated (as in formulae (7)) and finally transcendental equation can be solved directly for the complex permittivity.

### 3.2. *Measurements in resonant cavities*

Resonant cavities having axial symmetry are those most often used in the dielectric metrology. Cavities of this kind can operate on different modes but in practice one of the few first modes of the frequency spectrum is used.

*3.2.1. $TE_{01n}$ mode cavities.* Some of the most frequently employed modes are the $TE_{01n}$ ones that have been used for more than 60 years for measurements of the complex permittivity of disc samples (as shown in figure 8(*b*)) made of low-loss dielectrics [38–40] but also for measurements of

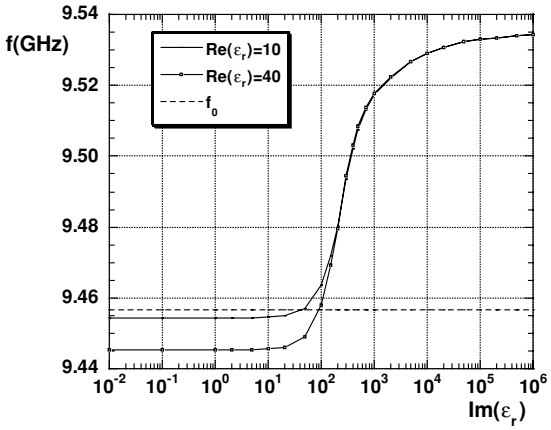


**Figure 11.** Resonant frequency versus imaginary part of permittivity for the $TE_{011}$ mode of a cylindrical cavity containing a dielectric disc sample. Parameters assumed in computations: $L = 25$ mm, $b = 25$ mm, $L_1 = 0$ mm, $h = 0.5$ mm. The dotted line corresponds to the $TE_{011}$ mode resonant frequency of the empty cavity.

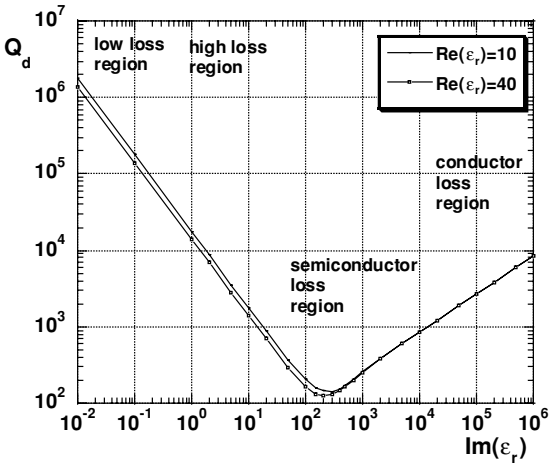


**Figure 12.** $Q$-factor due to dielectric losses versus imaginary part of permittivity for the $TE_{011}$ mode of a cylindrical cavity containing a dielectric disc sample.

conductivity of semiconductors and metals [41, 42]. A typical operating frequency range for the $TE_{01n}$ mode cavities is 8 GHz–40 GHz. One of the main advantages of the $TE_{01n}$ mode cavities is a circumferential electric field distribution that is tangential to a cylindrical sample inserted symmetrically in the cavity. As a result the electric field is continuous across dielectric–air interfaces that allows the air gap to be omitted without degradation of measurement uncertainties. Also the surface currents in the metal cavity walls are circumferential, so physical contact between the lateral surface and the cavity bottoms is not important, allowing easy construction of tunable cavities and easy sample insertion.

Let us now consider theoretical aspects of measurements of various materials in the $TE_{011}$ mode cylindrical cavity shown in figure 7(*b*) when the sample under test having arbitrary losses is situated directly on the bottom of the cavity. Results of the $TE_{011}$ mode resonant frequency and $Q$-factor due to dielectric loss evaluation are shown in figures 11 and 12.

Both resonant frequency and $Q$-factor due to dielectric losses exhibit very characteristic behaviour (common for any other resonator) as a function of the imaginary part of the

permittivity. In a low-loss dielectric region the resonant frequency is smaller than that for the empty cavity and the resonant frequency shift $(f_0 - f)$ depends on the real permittivity and thickness of the sample, but practically does not depend on losses. The inverse of the $Q$-factor due to dielectric losses in this region depends linearly on the dielectric loss tangent according to formulae (18) with a constant value of the electric energy filling factor $p_e$:

$$Q_d^{-1} = p_e \tan\delta. \tag{18}$$

For the low dielectric loss region the real part of the complex permittivity can be determined on the basis of the measured resonant frequency from a simplified transcendental equation where both the complex permittivity and the complex angular frequency have imaginary parts equal to zero. Evaluation of the dielectric loss tangent from the measured unloaded $Q$-factor value requires determination of all parasitic losses and electric energy filling factor in the sample. For a closed cavity conductor losses can be evaluated from formulae (14) and (15) assuming that the surface resistance of the cavity is known.

In fact the surface resistance in a closed cavity is always determined (at the resonant frequency of the empty cavity $f_0$) from the measured $Q$-factor of the empty cavity and then it is scaled to the frequency of the cavity containing the sample according to the formula

$$R_s(\omega) = R_s(\omega_0)\sqrt{\frac{\omega}{\omega_0}}. \tag{19}$$

The simplified approach of a low-loss sample gives results that are essentially the same as the complex angular frequency approach if the dielectric loss tangent of the sample is smaller than 0.1. If the losses become higher then the resonant frequency varies as a function of loss as seen in figure 11. As losses in the sample increase and the dielectric loss tangent becomes greater than 10 then both the resonant frequency and $Q_d$ predominantly depend on the imaginary part of the permittivity. In this region only the imaginary part of the permittivity can be determined. For relatively thin samples situated on the cavity bottom the electric energy filling factor in the sample is very small and the $Q$-factor depending on dielectric losses is greater than 100, so materials having arbitrary losses can be measured (at least in principle). On the other hand, for the imaginary part of the permittivity smaller than 0.1 (or dielectric loss tangent smaller than 0.01) the $Q$-factor due to dielectric losses becomes larger than $10^5$. Since $Q$-factors due to parasitic losses (conductor losses) in $TE_{011}$ mode cavities are typically in the range 15 000–30 000 (depending on frequency), so in such cases measurement uncertainties for low-loss dielectrics substantially increase. Measurements of low-loss dielectrics in $TE_{01n}$ mode cavities are possible either by using thicker samples (optimum thickness is half the wavelength or its multiple) or by elevating the sample to the position where the electric field approaches a maximum. In both cases electric energy filling factors in the sample become relatively large and high resolution of loss tangent determination can be obtained (of the order of $5 \times 10^{-5}$). Typical uncertainties of real permittivity determination employing $TE_{01n}$ mode cavities are the order of 0.5%. At frequencies lower than 8 GHz, the dimensions of $TE_{01n}$ mode cavities (and samples) become too large for practical applications so different resonators must be used.

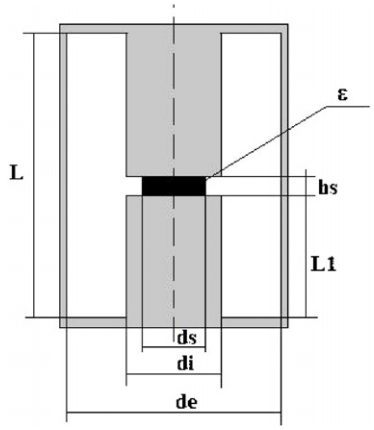


**Figure 13.** Schematic diagram of re-entrant cavity.

*3.2.2. $TM_{0n0}$ mode and re-entrant cavities.* In the past, the most commonly used cells operating in the frequency range from 2 GHz to 10 GHz were $TM_{010}$ mode cavities with rod samples as shown in figure 8(*a*) [16, 35, 37] and for frequencies from 50 MHz to 2 GHz were re-entrant cavities [16, 43, 44] as shown in figure 13. The electric field for both kinds of cells, the $TM_{010}$ mode cavity and the re-entrant cavity, has dominant axial component with maximum at the resonator axis while the magnetic field has only azimuthal component. As a result of such an electromagnetic field distribution the surface currents have a radial component on horizontal metal surfaces and an axial component on vertical surfaces of the cavities. Such a field distribution creates practical measurement difficulties. Firstly, any air gaps between sample and metal surfaces introduce significant errors in real permittivity determination (similar to those described for the coaxial transmission line method). Secondly, surface current distribution does not allow for easy disassembling of the resonant structure (because contact impedances reduce the $Q$-factor, and they tend not to be reproducible). This makes it necessary to have a door or lid in the cavity for sample insertion. In a re-entrant cavity the door is typically made in the lateral surface of the resonator and usually does not significantly change the $Q$-factor; for a $TM_{010}$ mode cavity a small lid is usually made in the centre of one or two cavity bottoms. Lids in the $TM_{010}$ mode cavity must be sufficiently small to get reproducible $Q$-factor values. Another possibility is to make small holes through the cavity and measure a sample that is longer than the height of the cavity. However, in such a case analysis of the structure becomes a problem. For a $TM_{010}$ mode cavity the transcendental equation is known only if the height of the sample is the same as the height of the cavity otherwise numerical analysis of the structure is necessary. For a re-entrant cavity the transcendental equation in a closed form does not exist for any case but rigorous mode-matching solutions are available [44]. $Q$-factors due to conductor losses for re-entrant cavities are typically in the range 1000–5000 and for $TM_{010}$ mode cavities in the range 2000–10 000. Since the electric energy filling factor in a re-entrant cavity is close to unity, resolution of dielectric loss tangent measurements in this cavity is also relatively high, i.e. of the order of $5 \times 10^{-5}$. Similar resolutions of dielectric loss tangent measurements can be obtained in $TM_{010}$ mode cavities if samples under

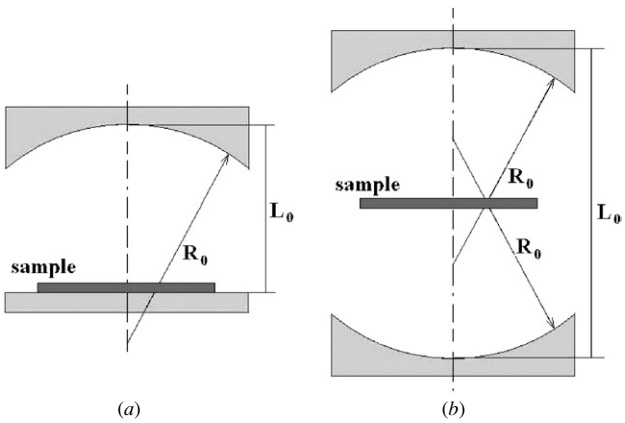


**Figure 14.** Fabry–Perot resonators used for measurements of laminar dielectrics.

test have sufficiently large diameter. Uncertainties of real permittivity determination for the re-entrant cavity and the $TM_{010}$ mode cavity might be strongly affected by the presence of air gaps. Errors associated with gaps increase as the aspect ratio of the sample (diameter to height) increases. If large permittivity samples are to be measured or/and their aspect ratio is large then the flat surfaces of samples must be metalized to obtain reasonable results. In re-entrant cavities uncertainties might also be affected by computational errors, as a rigorous transcendental equation for this cavity is not available. It should also be mentioned that in the same measurement set-up higher order $TM_{0n0}$ modes can be used for measurements of permittivity and dielectric loss tangent as a function of frequency. The transcendental equation for $TM_{0n0}$ modes remains the same as for the $TM_{010}$ mode. Resonators of this kind are commercially available with software for the complex permittivity determination.

Typical measurement uncertainties for real permittivity are about 0.5%–2% for $TM_{010}$ mode cavity and are about 1%–3% for re-entrant cavity.

*3.2.3. Fabry–Perot resonators.* Fabry–Perot resonators that are also known as open resonators are commonly used in the millimetre frequency range [45–52]. Typical geometries of Fabry–Perot resonators used for measurements of the complex permittivity of low-loss dielectrics are shown in figure 14. The electromagnetic field distribution for Fabry–Perot resonators is not accurately known but Gaussian beam approximation for the dominant family of $TEM_{00q}$ modes allows quite accurate measurements at the frequency of one of these modes where sample thickness is approximately the same as half the wavelength. The sample size must be sufficiently large to comprise full Gaussian beam energy; otherwise diffraction from sample edges may cause radiation losses. Also the size of the mirrors must be sufficiently large compared to the width of the Gaussian beam. The $Q$-factor for an empty Fabry–Perot resonator operating at millimetre wave frequencies is typically in the range 100 000–200 000 and increases with increasing mode index. On the other hand loss tangent resolution does not increase with increasing mode indices because in such a case electric energy filling factors in the sample decrease.

For a low permittivity sample having half the wavelength thickness the uncertainty of real permittivity can be as low as 0.5% but it can be larger for samples having arbitrary thickness. This is related to the approximate electromagnetic modelling of such structures. Loss tangent resolution in Fabry–Perot resonators is of the order of $1 \times 10^{-5}$ if the mode of interest does not interfere with spurious modes and radiation losses are not present. Full wave electromagnetic modelling of Fabry–Perot resonators is very difficult and at present none of the commercially available electromagnetic simulators gives satisfactory results for analysis of modes with large axial mode indices. The $Q$-factor of Fabry–Perot resonators can be increased at one single frequency by a factor of 5 or more employing so-called Bragg reflectors [57]. Due to their extremely high $Q$-factor such resonators seem to be ideal for precise measurements of the complex permittivity of gases.

### *3.3. Dielectric resonator structures*

For measurement techniques belonging to this category, the dominant part of the electromagnetic energy (usually more than 90%) is concentrated in the sample under test. A lot of specific techniques have been described that employ different modes and different measurement cells.

*3.3.1. $TE_{011}$ mode dielectric resonators.* Initially, the dielectric resonator technique for measurements of permittivity and losses of low-loss dielectrics was proposed by Hakki–Coleman [58] in 1960 employing the $TE_{011}$ mode of operation in a rod resonator terminated from both sides by conducting planes as shown in figure 10. Since its discovery, it has become one of the most accurate and the most frequently used techniques for measurements of permittivity and dielectric losses of solid materials. It is also known under different names as the Courtney [59] or parallel plate holder and it is also proposed as one of International Standards IEC techniques [60] for measurements of the complex permittivity of low-loss solids. It benefits from a very simple measurement configuration and easy access for introducing and removing specimens. For the $TE_{011}$ mode the applied electric field is continuous across the sample boundary, so air gaps between dielectric and metal planes do not play a significant role. As a result, high measurement accuracy of real permittivity can be achieved. This technique was applied by Courtney to measure both the complex permittivity and the complex scalar permeability of microwave ferrites. The main disadvantage of the originally described technique was that the surface resistance of metal plates could not be measured without the sample as in cavity methods. This difficulty has been overcome by measurements of two different $TE_{01n}$ modes on two dielectric samples made of the same material [61].

The $TE_{011}$ mode is one of several modes in the so-called 'trapped state', which means that radiation losses usually are not present for infinitely extended metal plates. Electromagnetic fields are evanescent in the air region (see figure 10) if the distance between the plates is smaller than half the wavelength corresponding to the resonant frequency. This happens if the aspect ratio of the dielectric sample is larger than a certain minimum value which depends on the permittivity of the sample. The lower the permittivity of the sample, the larger must be the aspect ratio of the sample to allow omitting the radiation losses. For example, for a

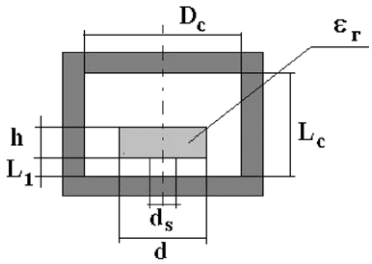


**Figure 15.** Schematic diagram of a $TE_{01\delta}$ mode dielectric resonator.

PTFE sample (with a permittivity of about 2.06) the minimum aspect ratio is about 2 but for alumina it is about 0.6. To avoid radiation losses in practice when dimensions of metal plates are finite the aspect ratio of the sample must be larger than those minimum values. It should be mentioned that in the case when metal plates are separated by a distance larger than half the wavelength, the $TE_{011}$ mode dielectric resonators have very low $Q$-factors predominantly affected by radiation. For example, for a sample having permittivity about 30 the $Q$-factor due to radiation losses is about 40. Under such conditions resonators cannot be used for measurements of low dielectric losses.

If an additional metal cylinder is introduced (creating a cylindrical cavity) in the parallel plate dielectric resonator operating in the trapped state then its resonant frequencies and $Q$-factors remain almost unaffected when the diameter of the cylinder is sufficiently large. Resonators of this kind may have some advantages over the parallel plate structure (especially for variable temperature measurements). Such resonators have been used for measurements of dielectric properties of several dielectric materials at cryogenic temperatures [62]. To minimize conductor losses high temperature superconductors were used as the end plates. A transcendental equation was derived for all modes in such a structure in the presence of uniaxial anisotropy of the sample allowing measurements of two permittivity tensor components. $TE_{011}$ mode dielectric resonators made of sapphire have been also used for measurements of the surface resistance of high temperature superconductors, e.g., [63]. Sapphire has dielectric loss tangent $<10^{-7}$ at cryogenic temperatures so the dielectric losses in the structure are negligible, the lateral metal wall losses are small and calculable and the surface resistance can be easily determined from equations (12)–(17) (see [63] for more details).

The uncertainty of the real permittivity measured in a Hakki–Coleman cell operating at ambient temperatures is usually of the order of 0.3% with dielectric loss tangent resolution of the order of $10^{-5}$. The latter value is limited by relatively large parasitic losses in the metal plates.

*3.3.2. $TE_{01\delta}$ mode dielectric resonators.* The effect of conductor losses on the loss tangent determination in the dielectric resonator structures can be mitigated if the sample under test is situated away from all conducting walls as shown in figure 15. Usually the $TE_{01\delta}$ mode is employed. The $TE_{01\delta}$ mode technique is one of the most accurate techniques for measurements of the dielectric loss tangent of isotropic low-loss dielectric materials but it can also be used for precise measurements of real permittivity [64, 65]. Manufacturers

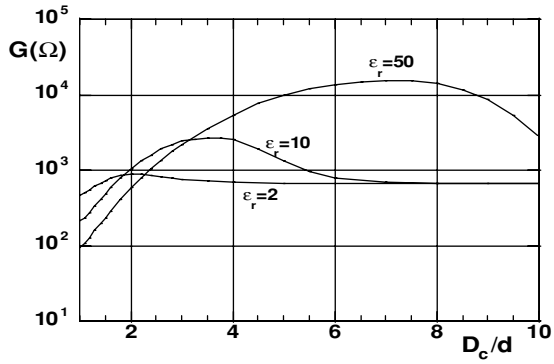


**Figure 16.** Geometric factor versus size of metal enclosure for $TE_{01\delta}$ mode dielectric resonators having different permittivities. $D_c/L_c = 2$, $L_1 = (L_c–h)/2$, dielectric support neglected.

of low-loss dielectric ceramics usually use this technique to measure only dielectric losses (as the inverse of the unloaded $Q$-factor of the structure shown in figure 15) avoiding analysis of the structure. They assume that for a metal cavity which is about three times larger than the dielectric sample conductor losses can be entirely neglected. As will be shown later such an assumption is not always valid. There are a lot of advantages associated with using the $TE_{01\delta}$ mode. The most important are the easy mode identification, small parasitic losses, especially for high permittivity samples, and the lack of mode degeneracy. Measurements of real permittivity are possible but its determination is more difficult than for parallel plate structure because of the lack of exact solutions of Maxwell's equation. However, if accurate numerical techniques are used the uncertainties of real permittivity determination associated with numerical modelling are smaller than those associated with dimensional uncertainties.

In figure 16 results of numerical computations of geometric factors versus size of metal enclosure are presented. It is seen that for an empty $TE_{011}$ cavity geometric factor value is about 660 Ω (which is visible as the limit for $D_c/d = 10$ for low permittivity samples) while for a high permittivity sample with $\varepsilon_r = 50$ geometric factor values exceed 10 000 Ω for $5 < D_c/d < 8.5$.

This means that conductor losses in the cavity for high permittivity samples have been reduced more than one order of magnitude compared to the empty cavity, allowing measurements of dielectric losses at least one order of magnitude smaller than in the $TE_{01n}$ mode cavities. Typical resolution of loss tangent resolution employing $TE_{01\delta}$ mode dielectric resonators technique with optimised enclosure is about $10^{-6}$ for high permittivity samples $\varepsilon_r > 20$ and uncertainty of real permittivity measurements of the order of 0.3% (similar for low and high permittivities). Low permittivity materials are more difficult to measure because for such materials the $TE_{01\delta}$ mode becomes one of the higher order modes in the frequency spectrum [65]. Only recently higher order quasi $TE_0$ modes in the structure shown in figure 15 have been employed for measurements of real permittivity and dielectric loss tangent as a function of frequency [66].

*3.3.3. Whispering gallery mode resonators.* To minimize further parasitic losses (conductor losses for closed structures

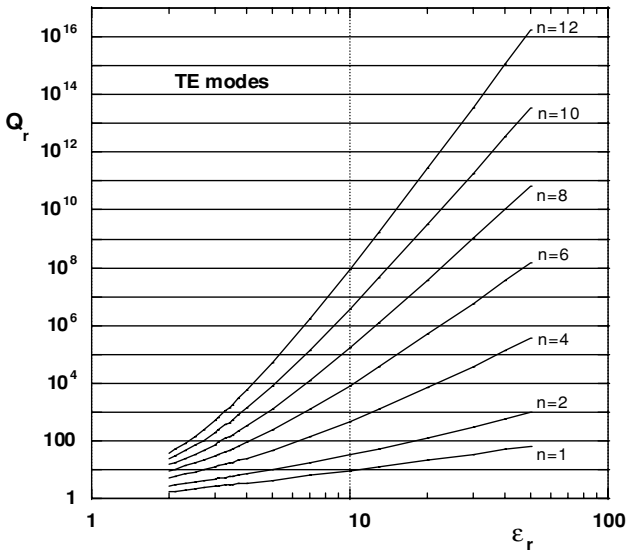


**Figure 17.** $Q$-factors due to radiation losses for $TE_0$ modes of isolated dielectric sphere.

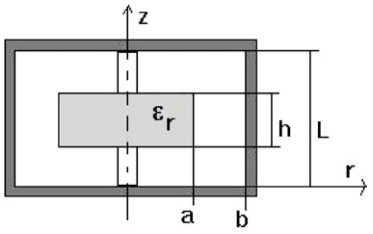


**Figure 18.** Schematic diagram of shielded cylindrical whispering gallery mode resonator. Supports can be made of metal.

or radiation losses for open structures) one can employ the modes having large azimuthal indices that can be excited in cylindrical or spherical dielectric samples. They are called whispering gallery modes because their electromagnetic field energy is concentrated near the lateral surface but inside the dielectric sample. The simplest structure of this kind is a spherical dielectric resonator in free space (figure 9(*a*)). Even for lossless dielectrics, transcendental equation (10) has solutions only for certain sets of complex angular frequencies due to radiation losses. Formally this is the consequence of properties of Hankel's function (they are complex valued for real arguments). Using the complex frequencies from the solution of (10), the $Q$-factor due to radiation can be computed as

$$Q_{\mathrm{r}} = \frac{\mathrm{Re}(\omega)}{2\,\mathrm{Im}(\omega)}. \qquad (20)$$

The results of the computations of radiation loss versus permittivity for the $TE_{n01}$ family of an open spherical dielectric resonator are shown in figure 17. As seen in figure 17, for large indices '$n$' and large values of permittivity, the $Q$-factor due to radiation approaches a very large value, e.g., $Q_{\mathrm{r}} \geqslant 10^8$ if $\varepsilon_{\mathrm{r}} \geqslant 10$ and $n \geqslant 12$. Even for low permittivity samples it is always possible to obtain $Q_{\mathrm{r}}$ arbitrarily large by choosing a sufficiently large index $n$. It means that even for extremely low-loss dielectrics the radiation losses for sufficiently high order whispering gallery modes are much smaller than dielectric losses.

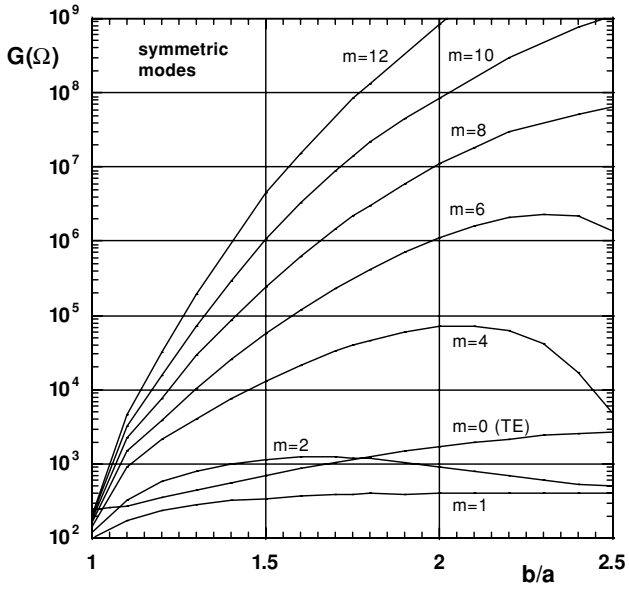


**Figure 19.** Geometric factors of symmetric modes versus normalized radius of perfect conductor shield for cylindrical resonator having permittivity $\varepsilon_{\mathrm{r}} = 10$. It was assumed that $L/h = b/a$.

For totally shielded resonators there are no radiation losses but conductor losses resulting from the surface resistance of the metal shield. The most popular shielded whispering gallery mode resonators are cylindrical ones situated in a cylindrical metal enclosure as shown in figure 18. The measurement cell is similar to that for the $TE_{01\delta}$ mode dielectric resonator but supports are usually made of metal and the sample is situated symmetrically in the cavity.

In general electromagnetic fields in cylindrical dielectric resonators are of hybrid nature, i.e. they have all six non-zero components (except axially symmetric modes). The modes in the structure shown in figure 18 can be divided into two categories: symmetric (with respect to the resonator plane of symmetry) for which the symmetry plane constitutes a perfect magnetic wall (S-modes) and antisymmetric for which the symmetry plane constitutes a perfect electric wall (N-modes). Such nomenclature is only valid if the shielded resonator possesses a plane of symmetry. For each category only two mode subscripts are used: the first one corresponding to the azimuthal index ($m$) and the second index '$i$' corresponding to the sequence of the particular mode on the frequency axis. Such nomenclature is very useful since it does not require complicated field plot analysis in order to distinguish between two unknown indices $n$ (radial) and $p$ (axial). Modes belonging to the primary WGMR families are therefore labelled as $S_{m,1}$ or $N_{m,1}$ and all other modes as $S_{m,i}$ or $N_{m,i}$. Modes with azimuthal index $m > 0$ of cylindrical resonators are always doubly degenerate.

The results of the numerical computations of the geometric factor employing a mode-matching technique are presented in figure 19. As seen in this figure the geometric factors increase rapidly with an increase of azimuthal mode index $m$, so it is always possible to choose this index so as to make the conductor losses negligible compared to the dielectric losses. One of the first papers describing the use of whispering gallery modes for measurements of

dielectric losses was published by Braginsky *et al* [69]. The authors of this paper measured the modes having the largest $Q$-factors on sapphire at cryogenic temperatures. Dielectric loss tangents were evaluated as the inverse of measured $Q$-factors. In later papers full numerical electromagnetic analysis of the structure was undertaken [68] and the whispering gallery mode technique used for measurements of two permittivity tensor components of several uniaxially anisotropic crystals [70]. This was done by employing two modes: one belonging to the quasi TE mode family (subscript $H$) and the other belonging to the quasi TM mode family (subscript $E$).

Real permittivities were evaluated as the solutions of the system of two nonlinear equations

$$\left.\begin{aligned} F_1(f^{(H)}, \varepsilon_\perp, \varepsilon_{||}) = 0 \\ F_2(f^{(E)}, \varepsilon_\perp, \varepsilon_{||}) = 0 \end{aligned}\right\}. \tag{21}$$

Once permittivities had been evaluated dielectric loss tangents were determined from the system of two linear equations

$$\left.\begin{aligned} Q_{(E)}^{-1} = p_{e\perp}^{(E)} \tan\delta_\perp + p_{e||}^{(E)} \tan\delta_{||} + R_S/G^{(E)} \\ Q_{(H)}^{-1} = p_{e\perp}^{(H)} \tan\delta_\perp + p_{e||}^{(H)} \tan\delta_{||} + R_S/G^{(H)} \end{aligned}\right\} \tag{22}$$

where $\tan\delta_\perp$ and $\tan\delta_{||}$ are the dielectric loss tangents perpendicular and parallel to the anisotropy axis; $p_{e\perp}^{(H)}$, $p_{e||}^{(H)}$, $p_{e\perp}^{(E)}$, $p_{e||}^{(E)}$ are the electric energy filling factors perpendicular (subscript $\perp$) and parallel (subscript $\|$) to the anisotropy axis of the resonant structure, for quasi-TM whispering gallery modes (superscript $E$) and quasi-TE whispering gallery modes (superscript $H$), and $G^{(E)}$ and $G^{(H)}$ are the geometric factors for quasi-TM and quasi-TE whispering gallery modes.

The main advantages of using whispering gallery modes are: practically unlimited resolution for dielectric loss tangent and the possibility of measurements of real permittivities for uniaxially anisotropic materials with uncertainties down to 0.1%. The main disadvantage is difficult mode identification and limited ability for measurements of materials having losses larger than $10^{-4}$.

## 4. Measurements of anisotropic materials with induced anisotropy

If samples under test are anisotropic they have to be oriented and cut with respect to their anisotropy axes. Natural anisotropy might be present in materials that do not possess symmetric crystallographic structure, but it might also be induced by mechanical stress or biasing electric or magnetic field. Measurement techniques for uniaxially anisotropic crystals have already been described in the former paragraphs. They employ two different modes excited in an oriented single-crystal sample. One of the most important materials belonging to the second group is microwave ferrites that exhibit gyromagnetic properties in the presence of biasing static magnetic field. As already mentioned the magnetic properties of ferrite under uniform bias along the $z$-axis can be described by Polder's tensor (5). The complex permittivity of polycrystalline ferrites is a scalar quantity, which does not depend on the static magnetic bias. At frequencies higher than ferromagnetic resonance magnetic losses in ferrites are usually

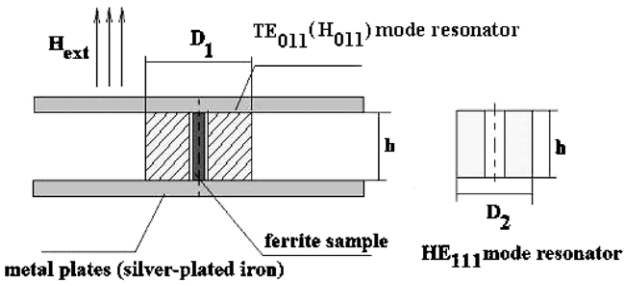


**Figure 20.** Measurement cells used for measurements of the permeability tensor of microwave ferrites versus static magnetic bias.

small so measurements of their properties requires application of resonant measurement cells. Several techniques have been used to measure ferrite properties that were described in journal papers, e.g., [35], and summarized in overview books on microwave ferrites (Gurevich [6], Baden-Fuller [71]). More recently a dielectric resonator technique was proposed that allows measurements of all three permeability tensor components on one rod-shaped ferrite sample [72]. Measurement cells for this technique are shown in figure 20. This technique uses three different modes in two dielectric resonators having the same height and internal diameter but different external diameters. One (larger) dielectric resonator operates on the $TE_{011}$ mode while the other on the (smaller) $HE_{111}$ mode. The $HE_{111}$ mode is the first mode in the trapped state for a parallel plate dielectric resonator. The external diameter of the smaller resonator is chosen such that its $HE_{111}$ mode resonant frequency (with the sample but without any bias) is approximately the same as the $TE_{011}$ mode resonant frequency of the larger resonator (with the sample but without any bias). Two resonators were used in order to mitigate the influence of frequency on the measurement results since permeability components are frequency dependent. Without any bias the $HE_{111}$ mode is doubly degenerate, which means that the two modes corresponding to the opposite circular polarizations, namely $HE_{111}^{+}$ and $HE_{111}^{-}$, have identical resonant frequencies. In practice however due to imperfect axial symmetry the two modes are split by a few MHz which gives rise to the measurement uncertainties. In the presence of a biasing field mode degeneracy is removed due to the appearance of an off-diagonal component of the permeability tensor. As this component increases the frequency difference between the two modes also increases as shown in figure 21. Resonant frequencies also depend on the other two permeability tensor components. At zero bias the resonant frequencies of the degenerate $HE_{111}$ mode and $TE_{011}$ mode depend on two unknowns, namely the scalar permeability and the scalar permittivity of the ferrite sample, so the two unknowns can be determined from the system of two transcendental equations

$$\left.\begin{aligned} F_{10}(\mu_d, \varepsilon, f_{\mathrm{HE}}) = 0 \\ F_{30}(\mu_d, \varepsilon, f_{\mathrm{HE}}) = 0 \end{aligned}\right\}. \tag{23}$$

When the permittivity is known the three permeability tensor components at arbitrary fixed bias can be determined from the system of three transcendental equations

$$\left.\begin{aligned} F_1(\mu, \kappa, \mu_z, \varepsilon, f_{\mathrm{HE}+}) = 0 \\ F_2(\mu, \kappa, \mu_z, \varepsilon, f_{\mathrm{HE}+}) = 0 \\ F_3(\mu, \kappa, \mu_z, \varepsilon, f_{\mathrm{TE}}) = 0 \end{aligned}\right\}. \tag{24}$$

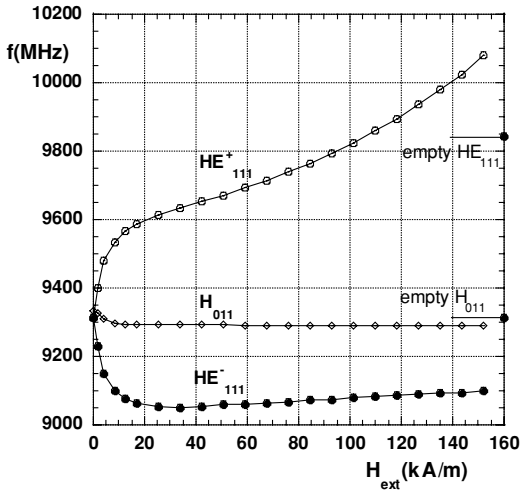


**Figure 21.** Measured frequencies of three different modes of two cylindrical resonators containing a YIG sample versus static magnetic field bias.

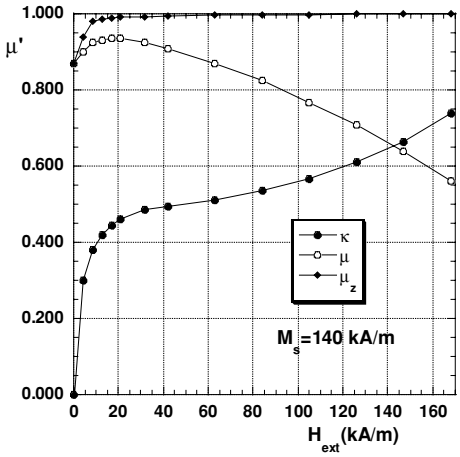


**Figure 22.** Real parts of three permeability tensor components of a YIG sample versus static magnetic field bias.

Finally three magnetic loss tangent components can be found on the basis of measured unloaded $Q$-factors of three different modes as solutions of the system of linear equations

$$\left.\begin{aligned} Q_1^{-1} &= p_{1\varepsilon}\tan\delta_\varepsilon + p_{1\mu}\tan\delta_\mu + p_{1\kappa}\tan\delta_\kappa \\ &\quad + p_{1\mu z}\tan\delta_{\mu z} + Q_{1c}^{-1} + Q_{1d}^{-1} \\ Q_2^{-1} &= p_{2\varepsilon}\tan\delta_\varepsilon + p_{2\mu}\tan\delta_\mu + p_{2\kappa}\tan\delta_\kappa \\ &\quad + p_{2\mu z}\tan\delta_{\mu zz} + Q_{2c}^{-1} + Q_{2d}^{-1} \\ Q_3^{-1} &= p_{3\varepsilon}\tan\delta_\varepsilon + p_{3\mu}\tan\delta_\mu + p_{3\kappa}\tan\delta_\kappa \\ &\quad + p_{3\mu z}\tan\delta_{\mu zz} + Q_{3c}^{-1} + Q_{3d}^{-1} \end{aligned}\right\}. \tag{25}$$

Results of the determination of the real parts of the permeability tensor versus bias for yttrium iron garnet (YIG) are shown in figure 22. More details about this technique (frequency corrections for individual tensor components) can be found in [72]. Measurement uncertainties for real permeability components using this technique are typically of the order of 1% and the magnetic loss tangent resolution is about $5 \times 10^{-5}$.

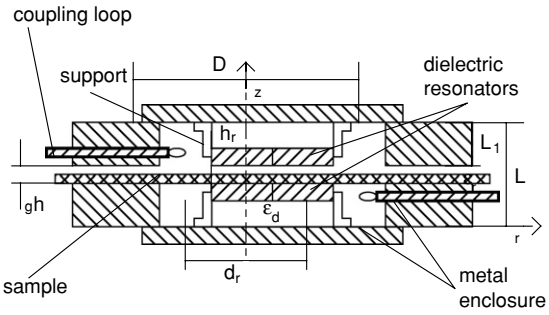


**Figure 23.** Schematic diagram of a split dielectric resonator fixture.

## 5. Resonators for measurements of laminar dielectric materials and thin films deposited on dielectric substrates

Advances in numerical computations of electromagnetic fields [73] have enabled the implementation of resonant structures with more complicated geometry. Hence the geometry of a resonant cavity can be chosen to suit materials having specific shape and dimensions. The split post dielectric resonator (SPDR) is a good example of such an approach as it has been developed specifically for measurement of laminar dielectrics [74–76]. The geometry of a split dielectric resonator is shown in figure 23. Currently the SPDR is one of the most convenient and accurate techniques for determination of permittivity and loss tangent of PWB and LTCC materials and ferrite substrates [78] in the frequency range from 1 GHz to 30 GHz.

The main advantages of split post dielectric resonators are: arbitrary shape of samples under test (they only need to have uniform thickness), smaller dimensions than for metal cavity resonators, and possibility of measurement of various materials including thin film ferroelectrics [79]. With properly chosen sample thickness it is possible to resolve dielectric loss tangents to approximately $2 \times 10^{-5}$ and $Q$-factor measurements with an accuracy of 1%. For well-machined laminar specimens the uncertainty in permittivity measurements using the SPDR is about 0.3% [77].

At frequencies higher than 20 GHz the size of split post dielectric resonators becomes very small and their $Q$-factors also become smaller than at lower frequencies (about 7000 at 20 GHz). At millimetre wave frequencies split metal cavity techniques can be alternatively used for non-destructive testing of laminar specimens [80–82].

## 6. Summary

This paper has overviewed only a small fraction of the available techniques for measurement of material properties at microwave frequencies. A lot of techniques exist that were not mentioned in this paper that utilize microstrip, stripline and coplanar waveguide cells (both transmission line and resonant ones). General properties of such structures are similar to those described in this paper. Typically transmission/reflection techniques are useful for characterization of high and medium loss materials and resonant techniques can be in principle used for measurements of materials having arbitrary losses. On the other hand, resonant techniques are in most cases

limited to one fixed frequency (although sometimes a few different modes can be used in one measurement cell) while transmission/reflection techniques can typically operate at broad frequency bands. One of the most important issues for all techniques is their sensitivity to the presence of air gaps between the sample and other parts of the measurement cell. Resolution of loss tangent measurements for arbitrary technique is associated with the presence of parasitic losses in measuring cells. They must be calculable and relatively small with respect to the losses in the sample in order to measure precisely losses in the material under test. Determination of both permittivity and permeability for magnetic materials and measurements of anisotropic materials always requires measurements of at least the same number of parameters as the number of unknowns. Precise determination of permittivity at microwave frequencies also requires full electromagnetic modelling of measurement cells, which is still one of the most challenging problems in microwave materials metrology.

## References


[1] Von Hippel A 1954 *Dielectric Materials and Applications* (New York: Wiley/The Technology Press of MIT) (new edition published 1995) (Dedham, MA: Artech House)

[2] Birch J R and Clarke R N 1982 Dielectric and optical measurements from 30 to 1000 GHz *Radio Electron. Eng.* **52** 565–84

[3] Anderson J C 1964 *Dielectrics (Science Paperbacks, Modern Electrical Studies)* (London: Chapman and Hall)

[4] Clarke R N 2004 *A Guide to the Characterisation of Dielectric Materials at RF and Microwave Frequencies* (Teddington: NPL)

[5] Burfoot J C 1967 *Ferroelectrics: An Introduction to the Physical Principles* (London: Van Nostrand-Reinhold)

[6] Gurevich A G 1963 *Ferrites at Microwave Frequencies* (New York: Consultants Bureau Enterprises Inc.)

[7] Nicolson A M and Ross G F 1970 Measurement of the intrinsic properties of materials by time domain techniques *IEEE Trans. Instrum. Meas.* **19** 377–82

[8] Weir W B 1974 Automatic measurement of complex dielectric constant and permeability at microwave frequencies *Proc. IEEE*

[9] Baker-Jarvis J, Vanzura E J and Kissick W A 1990 Improved technique for determining complex permittivity with the transmission/reflection method *IEEE Trans. Microw. Theory Tech.* **38** 1096–103

[10] ASTM D 5568.01 1995 Standard test method for measuring relative complex permittivity and relative magnetic permeability of solid materials at microwave frequencies (American Society for the Testing of Materials) (http://www.astm.org)

[11] UTE Standard 26-295 1999 *Mesure de la permittivité et de la permeabilité de materiaux homogenes et isotropes a pertes dans le domaine des micro-ondes. Methode de mesure en guide coaxial circulaire* (France: UTE (Union Technique de l'Electricite et de la Communication)) C26-295 (http://www.ute-fr.com)

[12] Boughriet A H, Legrand C and Chapoton A 1997 Noniterative stable transmission/reflection method for low-loss material complex permittivity determination *IEEE Trans. Microw. Theory Tech.* **45** 52–7

[13] Jenkins S, Hodgetts T E, Clarke R N and Preece A W 1990 Dielectric measurements on reference liquids using automatic network analysers and calculable geometries *Meas. Sci. Technol.* **1** 691–702

[14] Gregory A P and Clarke R N 2001 Tables of complex permittivity of dielectric reference liquids at frequencies up to 5 GHz *NPL Report CETM* 33 (Teddington: NPL)

[15] Grigas J 1996 *Spectroscopy of Ferroelectrics and Related Materials* (Amsterdam: Gordon and Breach)

[16] Brandt A 1963 *Investigations of Dielectrics at Ultra High Frequencies* (Moscow: GIFML) (in Russian)

[17] Stuchly M A and Stuchly S S 1980 Coaxial line reflection methods for measuring dielectric properties of biological substances at radio and microwave frequencies—a review *IEEE Trans. Instrum. Meas.* **29** 176–83

[18] Mosig J R, Besson J-C E, Gex-Fabry M and Gardiol F E 1981 Reflection of an open-ended coaxial line and application to non-destructive measurement of materials *IEEE Trans. Instrum. Meas.* **30** 46–51

[19] Anderson L S, Gajda G B and Stuchly S S 1986 Analysis of open-ended coaxial line sensor in layered dielectric *IEEE Trans. Instrum. Meas.* **35** 13–8

[20] Hodgetts T E 1989 The open-ended coaxial line: a rigorous variational treatment *Royal Signals and Radar Establishment Memorandum*, Royal Signals and Radar Establishment, No 4331

[21] Baker-Jarvis J, Janezic M D, Domich P D and Geyer R G 1994 Analysis of an open-ended coaxial probe with lift-off for nondestructive testing *IEEE Trans. Instrum. Meas.* **45** 711–8

[22] Sphicopoulos T, Teodoridis V and Gardiol F E 1985 Simple nondestructive method for the measurement of material permittivity *J. Microw. Power* **20** 165–72

[23] Bakhtiari S, Ganchev S and Zoughi R 1993 Open-ended rectangular waveguide for nondestructive thickness measurement and variation detection of lossy dielectric slab backed by a conducting plate *IEEE Trans. Instrum. Meas.* **42** 19–24

[24] Clarke R N, Gregory A P, Hodgetts T E, Symm G T and Brown N 1995 Microwave measurements upon anisotropic dielectrics—theory and practice *Proc. 7th Int. British Electromagnetic Measurements Conf. (BEMC)* Paper 57 (Teddington: NPL)

[25] Kogelnik H and Li T 1966 Laser beams and resonators *Proc. IEEE* **54** 1312–29

[26] Clarricoats P J B and Olver A D 1984 *Corrugated Horns for Microwave Antennas (IEE Electromagnetic Waves Series 18)* (London: Peter Peregrinus)

[27] Wylde R J 1984 Millimetre-wave Gaussian beam modes optics and corrugated feed horns *Proc. IEE H* **131** 258–62

[28] Afsar M N, Birch J R and Clarke R N 1986 The measurement of the properties of materials *Proc. IEEE* **74** 183–98

[29] Cook R J and Rosenberg C B 1979 Measurements of the complex refractive index of isotropic and anisotropic materials at 35 GHz using a free-space microwave bridge *J. Phys. D: Appl. Phys.* **12** 1643–52

[30] Stone N W B, Harries J E, Fuller D W E, Edwards J G, Costley A E, Chamberlain J, Blaney T G, Birch J R and Bailey A E 1975 Electrical standards of measurement: Part 3. Submillimetre-wave measurements and standards *Proc. IEEE* **122** 1054–70

[31] Campbell C K 1978 Free space permittivity measurements on dielectric materials at millimeter wavelengths *IEEE Trans. Instrum. Meas.* **27** 54–8

[32] Shimbukuro F I, Lazar L, Chernick M R and Dyson H B 1984 A quasi-optical method for measuring the complex permittivity of materials *IEEE Trans. Microw. Theory Tech.* **32** 659–65

[33] Qureshi W M A, Hill L D, Scott M and Lewis R A 2003 Use of a Gaussian beam range and reflectivity arch for characterisation of random panels for a naval application *Proc. Int. Conf. on Antennas and Propagation (ICAP) (University of Exeter)* (London: IEE) pp 405–8

[34] Gagnon N, Shaker J, Berini P, Roy L and Petosa A 2003 Material characterization using a quasi-optical measurement system *IEEE Trans. Instrum. Meas.* **52** 333–36

[35] Bussey H E and Steinert L A 1958 Exact solution for a gyromagnetic sample and measurements on a ferrite *IRE Trans. Microw. Theory Tech.* **6** 72–6

[36] Li S, Akyel C and Bosisio R G 1981 Precise calculations and measurement on the complex dielectric constant of lossy materials using $TM_{010}$ perturbation techniques *IEEE Trans. Microw. Theory Tech.* **29** 1041–8

[37] Risman P O and Ohlsson T 1975 Theory for and experiments with a $TM_{020}$ applicator *J. Microw. Power* **10** 271–80

[38] Horner F, Taylor T A, Dunsmuir R, Lamb J and Jackson W 1946 Resonance methods of dielectric measurement at centimetre wavelengths *J. IEE* **93** (Part III) 53–68

[39] Cook R J, Jones R G and Rosenberg C B 1974 Comparison of cavity and open-resonator measurements of permittivity and loss angle at 35 GHz *IEEE Trans. Instrum. Meas.* **23** 438–42

[40] Stumper U 1973 A TE01n cavity resonator method to determine the complex permittivity of low loss liquids at millimetre wavelengths *Rev. Sci. Instrum.* **44** 165–9

[41] Krupka J and Milewski A 1978 Accurate method of the measurement of complex permittivity of semiconductors in $H_{01n}$ cylindrical cavity *Electron. Technol.* **11** 11–31

[42] Dmowski S, Krupka J and Milewski A 1980 Contactless measurement of silicon resistivity in cylindrical $TE_{01n}$ mode cavities *IEEE Trans. Instrum. Meas.* **29** 67–70

[43] Parry J V 1951 The measurement of permittivity and power factor of dielectrics at frequencies from 300 to 600 Mc/s *Proc. Inst. Electr. Eng.* **98** 303–11

[44] Kączkowski A and Milewski 1980 A high-accuracy wide-range measurement method for determination of complex permittivity in reentrant cavity: Part A. Theoretical analysis of the method *IEEE Trans. Microw. Theory Tech.* **28** 225–8

[45] Cullen A L and Yu P K 1971 The accurate measurement of permittivity by means of an open resonator *Proc. R. Soc. Lond.* A **325** 493–509

[46] Jones R G 1976 Precise dielectric measurements at 35 GHz using a microwave open-resonator *Proc. IEE* **123** 285–90

[47] Clarke R N and Rosenberg C B 1982 Fabry–Perot and open resonators at microwave and millimeter wave frequencies, 2–300 GHz *J. Phys. E: Sci. Instrum.* **15** 9–24

[48] Hirvonen T M, Vainikainen P, Łozowski A and Raisanen A V 1996 Measurement of dielectrics at 100 GHz with an open resonator connected to a network analyser *IEEE Trans. Microw. Theory Tech.* **45** 780–6

[49] Lynch A C and Clarke R N 1992 Open resonators: improvement of confidence in measurement of loss *IEEE Proc.* A **139** 221–5

[50] Heidinger R, Schwab R and Königer F 1998 A fast sweepable broad-band system for dielectric measurements at 90–100 GHz *23rd Int. Conf. on Infrared and Millimeter Waves (Colchester, UK)* ed T J Parker pp 353–4

[51] Heidinger R, Dammertz G, Meiera A and Thumm M K 2002 CVD diamond windows studied with low- and high-power millimeter waves *IEEE Trans. Plasma Sci.* **30** 800–7

[52] Danilov I and Heidinger R 2003 New approach for open resonator analysis for dielectric measurements at millimeter wavelengths *J. Eur. Ceram. Soc.* **23** 2623–6

[53] Kobayashi Y, Fukuoka N and Yoshida S 1981 Resonant modes for a shielded dielectric rod resonator *Electron. Commun. Japan* **64-B** 46–51

[54] Julien A and Guillon P 1986 Electromagnetic analysis of spherical dielectric shielded resonators *IEEE Trans. Microw. Theory Tech.* **34** 723–29

[55] Kobayashi Y, Aoki Y and Kabe Y 1985 Influence of conductor shields on the $Q$-factors of a $TE_0$ dielectric resonator *IEEE Trans. Microw. Theory Tech.* **33** 1361–6

[56] Kajfez D and Guillon P (ed) 1990 *Dielectric Resonators* (Oxford, MS: Vector Fields)

[57] Krupka J, Cwikla A, Mrozowski M, Clarke R N and Tobar M E 2005 High $Q$-factor microwave Fabry–Perot resonator with distributed Bragg reflectors *IEEE Trans. Ultrason. Ferroelectr. Freq. Control* **52** 1443–51

[58] Hakki B W and Coleman P D 1960 A dielectric resonator method of measuring inductive capacities in the millimeter range *IEEE Trans. Microw. Theory Tech.* **8** 402–10

[59] Courtney W E 1970 Analysis and evaluation of a method of measuring the complex permittivity and permeability of microwave insulators *IEEE Trans. Microw. Theory Tech.* **18** 476–85

[60] IEC 61338, Sections 1-1, 1-2 and 1-3 (1996–2003) Waveguide type dielectric resonators: Part 1. General information and test conditions—Section 3. Measurement method of complex permittivity for dielectric resonator materials at microwave frequency (www.iec.ch)

[61] Kobayashi Y and Katoh M 1985 Microwave measurement of dielectric properties of low-loss materials by the dielectric rod resonator method *IEEE Trans. Microw. Theory Tech.* **33** 586–92

[62] Krupka J, Geyer R G, Kuhn M and Hinken J 1994 Dielectric properties of single crystal $Al_2O_3$, $LaAlO_3$, $NdGaO_3$, $SrTiO_3$, and MgO at cryogenic temperatures and microwave frequencies *IEEE Trans. Microw. Theory Tech.* **42** 1886–90

[63] Krupka J, Klinger M, Kuhn M, Baranyak A, Stiller M, Hinken J and Modelski J 1993 Surface resistance measurements of HTS films by means of sapphire dielectric resonators *IEEE Trans. Appl. Supercond.* **3** 3043–8

[64] Takamura H, Matsumoto H and Wakino K 1989 Low temperature properties of microwave dielectrics *Proc. 7th Meeting on Ferroelectric Materials and Their Applications, Japan. J. Appl. Phys.* **28** (Suppl. 28-2) 21–3

[65] Krupka J, Derzakowski K, Riddle B and Baker-Jarvis J 1998 A dielectric resonator for measurements of complex permittivity of low loss dielectric materials as a function of temperature *Meas. Sci. Technol.* **9** 1751–6

[66] Krupka J, Huang W-T and Tung M-J 2005 Complex permittivity measurements of low loss microwave ceramics employing higher order quasi TE0np modes excited in a cylindrical dielectric sample *Meas. Sci. Technol.* **16** 1014–20

[67] Krupka J, Cros D, Aubourg M and Guillon P 1994 Study of whispering gallery modes in anisotropic single crystal dielectric resonators *IEEE Trans. Microw. Theory Tech.* **42** 56–61

[68] Krupka J, Derzakowski K, Abramowicz A, Tobar M E and Geyer R G 1999 Whispering gallery modes for complex permittivity measurements of ultra-low loss dielectric materials *IEEE Trans. Microw. Theory Tech.* **47** 752–9

[69] Braginsky V, Ilchenko V S and Bagdassarov Kh S 1987 Experimental observation of fundamental microwave absorption in high quality dielectric crystals *Phys. Lett.* A **120** 300–5

[70] Krupka J, Derzakowski K, Tobar M E, Hartnett J and Geyer R G 1999 Complex permittivity of some ultralow loss dielectric crystals at cryogenic temperatures *Meas. Sci. Technol.* **10** 387–92

[71] Baden-Fuller A J 1987 *Ferrites at Microwave Frequencies (IEE Electromagnetic Wave Series No 23)* (London: Peter Peregrinus)

[72] Krupka J 1991 Measurements of all permeability tensor components and the effective linewidth of microwave ferrites using dielectric ring resonators *IEEE Trans. Microw. Theory Tech.* **39** 1148–57

[73] Maj Sz and Pospieszalski M 1984 A composite multilayered cylindrical dielectric resonator *IEEE MTT-S Int. Microwave Symp. Dig.* pp 190–2

[74] Krupka J and Maj S 1986 Application of $TE_{01\delta}$ mode dielectric resonator for the complex permittivity measurements of semiconductors *CPEM'86 Conf. Dig.* pp 154–5

[75] Nishikawa T, Wakino K, Tanaka H and Ishikawa Y 1988 Precise measurement method for complex permittivity of microwave substrate *CPEM'88 Conf. Dig.* pp 154–5

[76] Krupka J, Geyer R G, Baker-Jarvis J and Ceremuga J 1996 Measurements of the complex permittivity of microwave circuit board substrates using split dielectric resonator and reentrant cavity techniques *DMMA'96 Conf. Dig.* pp 21–4

[77] Krupka J, Gregory A P, Rochard O C, Clarke R N, Riddle B and Baker-Jarvis J 2001 Uncertainty of complex permittivity measurements by split-post dielectric resonator technique *J. Eur. Ceram. Soc.* **21** 2673–6

[78] Krupka J, Gabelich S A, Derzakowski K and Pierce B M 1999 Comparison of split-post dielectric resonator and ferrite disk resonator techniques for microwave permittivity measurements of polycrystalline yttrium iron garnet *Meas. Sci. Technol.* **10** 1004–8

[79] Krupka J, Huang W T and Tung M J 2005 Complex permittivity measurements of thin ferroelectric films employing split post dielectric resonator *11th Int. Meeting on Ferroelectricity (Foz do Iguacu, Brazil, 5–9 Sept. 2005)*

[80] Kent G 1996 Nondestructive permittivity measurements of substrates *IEEE Trans. Instrum. Meas.* **45** 102–6

[81] Janezic M D and Baker-Jarvis J 1999 Full-wave analysis of a split-cylinder resonator for nondestructive permittivity measurements *IEEE Trans. Microw. Theory Tech.* **47** 2014–20

[82] Janezic M D, Krupka J and Baker-Jarvis J 2001 Non-destructive permittivity measurements of dielectric substrates using split-cylinder and split-post resonators *Dig. of Int. Conf. APTADM'2001* pp 116–8